Chemical Papers (2024) 78:2855–2865
https://doi.org/10.1007/s11696-023-03276-3

ORIGINAL PAPER

Titanium carbide MXene/silver nanostars composite as SERS substrate for thiram pesticide detection

Nur Nazhifah Yusoff[1] · Farah Shahadah Nor Azmi[1] · Norhayati Abu Bakar[1,2] · Tengku Hasnan Tengku Abdul Aziz[1] · Joseph George Shapter[2]

Received: 22 September 2023 / Accepted: 11 December 2023 / Published online: 23 January 2024

Abstract

Two-dimensional transition metal carbonitrides, $Ti_3C_2T_x$ MXene nanosheets, have drawn much attention due to their unique optical properties. These materials have huge potential to be employed as surface-enhanced Raman scattering (SERS) substrates. Herein, to combine the benefits of metal nanoparticles and MXene as SERS substrates, we prepared composite SERS films with different volume ratios composed of $Ti_3C_2T_x$ MXene with silver nanostars (AgNs) as a promising SERS substrate for detection of pesticides. These SERS films were prepared via a drop-casting technique. The SERS activities of the MXene/AgNs composites were evaluated through detection of the thiram pesticide. MXene/AgNs exhibited the highest SERS intensity compared to MXene or AgNs substrate alone. Sampling from 20 different areas and samples of the substrate gave very consistent SERS signals. The MXene/AgNs substrate shows good stability for 1 month when stored in a small transparent container with silica gel. The MXene/AgNs SERS substrate exhibits excellent sensitivity able to detect thiram concentrations as low as 10^{-8} M which also having low a relative standard deviation (RSD) value for reproducibility and stability over a significant period.

Keywords MXene nanosheets · Silver nanostar · Surface-enhanced Raman scattering · Thiram fungicide

Introduction

Pesticide residues are a global threat to human health and environmental safety (Yuan et al. 2011). Pesticides are chemicals substances used to eliminate or control weeds and other pests (Qing Li et al. 2006; Yuan et al. 2011). Chemically related pesticides are divided into five classes based on their chemical structure and functionalities: neonicotinoid, organophosphate, dithiocarbamate, organochlorine and pyrethoid (Lim et al. 2016). Dithiocarbamates are a group of organosulfur compounds that are usually used as fungicides. These fungicides are classified by World Health Organization (WHO) as hazardous (Dao et al. 2019). Thiram is one of the types of fungicide that is frequently used to prevent crop damage either in the field or during transport and storage of the crop. The excessive use of thiram can contaminate soil, leak into groundwater, or be dispersed as dust in the air, leading to high toxicity for human skin (Liu et al. 2019; Bhavya et al. 2020). Thiram can be detected using a variety of techniques, including gas chromatography/mass spectrometry, UV–visible spectrophotometry, high-performance liquid chromatography, liquid chromatography-atmospheric pressure chemical ionization mass spectrometry, and chemiluminescence analysis (Llorent-Martínez et al. 2011; Chang et al. 2016; Wang et al. 2019). However, all these methods require multiple steps of sample pretreatment and have complicated operating procedures. Therefore, it is very important to conduct research on detection techniques that do not have a complex sample preparation while having strong specificity, rapid detection times and good sensitivity.

Surface-enhanced Raman spectroscopy (SERS) is nondestructive analytical method that can be employed to detect thiram. Due to its high sensitivity, distinct detection specificity, and fast response, SERS has been widely employed for analyte (single molecule or biomolecule) detection

✉ Norhayati Abu Bakar
norhayati.ab@ukm.edu.my

[1] Institute of Microengineering and Nanoelectronic (IMEN), Universiti Kebangsaan Malaysia, 43600 Bangi, Selangor, Malaysia

[2] Australian Institute for Bioengineering and Nanotechnology, University of Queensland, St. Lucia, Brisbane, QLD 4072, Australia

(Zhang et al. 2014; Guo et al. 2015). SERS, known as a surface-sensitive method, can enhance Raman scattering from molecules adsorbed on rough metal surfaces or nanostructures. In general, SERS enhancements come from two mechanisms, namely an electromagnetic (EM) mechanism and a chemical (CM) mechanism (Zhang et al. 2014; Chu et al. 2017; Xia 2018). Surface plasmon excitation of noble metals increases the surface electromagnetic field in the EM mechanism, whereas in the CM mechanism charge transfer between the target molecules and substrate is involved (Uskoković-Marković et al. 2017). Therefore, to provide the best enhancement of signal, it is essential to have a substrate that can support both mechanisms.

Due to their straightforward, environmentally friendly synthesis and ability to increase EM properties, silver and gold nanoparticles are two materials that are often manufactured to make SERS substrates. These two materials have been manufactured in various forms, like a nanostars, to enhance the SERS signal. A previous study by Bhavy et al. investigated the use of silver nanocubes and nanowires for SERS applications (Bhavya et al. 2020). They found that silver nanocubes give better enhancement compared to silver nanowires. In our study, we aimed to replicate and expand upon their findings but used silver nanostars (AgNs) instead of nanocubes. The pointed tip structure of AgNs allows them to generate powerful hot spots without the need for any aggregation techniques. AgNs do contribute to EM enhancement, but to effectively detect analytes with great sensitivity, reproducibility and stability, a SERS substrate that can also contribute to EM and CM enhancement must be fabricated.

Several research studies have been conducted to explore the potential of SERS technique for the detection of thiram (Zhu et al. 2018; Bhavvya et al. 2022; Shafi et al. 2022). For example, a study published in the Journal Food Chemistry in 2022 demonstrated that the SERS technique could be used to detect thiram residues in different fruit and vegetable peels (Picone et al. 2022). In this study, silver nanoparticles were used as SERS substrates. The SERS spectra of thiram were recorded, and a detection limit of 2 pg/cm^2 was achieved. Another study showed that SERS could be used to detect thiram in soil samples (Shafi et al. 2022). In this study, graphene-covered silver nanoparticles were used as SERS substrates and a detection limit of 0.005 ppm was achieved.

Due to its distinct physical, chemical, optical and electrical features, the MXene family of two-dimensional (2D) materials has attracted a great deal of attention. These materials are made of transition-metal carbides, nitrides, and carbonitrides (Garg et al. 2020; Wang 2021; Wang et al. 2021). The first prepared $Ti_3C_2T_x$ MXene, where T_x stands for different functional groups on the surface terminations (–OH, –F, and –O), has been shown to be a successful substrate. In one study, researchers synthesized seven types of MXene: Nb_2C, Mo_2C, Ti_2C, V_2C, Ti_3C_2, Mo_2TiC_2, and Ti_3CN (Shevchuk et al. 2022). They found that Ti_3C_2 and Ti_2C show the highest SERS enhancement. MXene is suitable as SERS substrate for several reasons. The large surface area of MXene allows the adsorption of target molecules, and the transfer of charges between the molecules and MXenes should result in the generation of CM enhancement on SERS-active nanostructures. There are several research studies that have investigated the use of MXene in SERS applications. One study evaluated the SERS performance of the MXene using organic dye Rhodamine 6G. The results showed that the MXene substrate had a detection limit of 10^{-7} M (Sarycheva et al. 2017). Another study explored the use of MXene as a SERS substrate for detection of chlorpromazine in human biological fluids like urine and saliva (Barveen et al. 2021). The researchers synthesized MXene with incorporation of gold nanoparticles to enhance the SERS effect and achieved a detection limit at 3.92×10^{-11} M. These findings demonstrate the high sensitivity of MXene-based SERS substrates for detecting environmental analytes.

Herein, we have fabricated AgNs, MXene SERS substrates and introduced MXene in the AgNs system to improve the thiram signal. To date, there are no reports of a SERS substrate fabrication of MXene using anisotropic AgNs for thiram detection that potentially lead to larger electromagnetic field enhancement. MXene has a large surface area while AgNs has high number of hot spots due to its spike structure. Inspired by these properties, we believe both properties can give best SERS enhancement. Thiram is used to evaluate the MXene/AgNs substrate's analytical potential and SERS performance as a composite SERS substrate. The results demonstrate that the MXene/AgNs composite is suitable for practical application in the detection of pesticides.

Experimental

The materials for $Ti_3C_2T_x$ MXene preparation are titanium aluminum carbide (Ti_3AlC_2) MAX phase (bulk material, Carbon-Ukraine Ltd), lithium fluoride (LiF) (98.5%, 325 mesh powder, Alfa Aesar) and hydrochloric acid (HCl) (32%, RCI Labscan). The chemicals for the synthesized AgNs are silver nitrate ($AgNO_3$) (99%, Sigma-Aldrich), hydroxylamine (HA) (50wt. % in water, Sigma-Aldrich), trisodium citrate dehydrate (TC) (99%, Sigma-Aldrich) and sodium hydroxide (NaOH) (98.0%, Chem-Supply Pty Ltd). Thiram-pestanal (Analytical standard, Sigma-Aldrich) was used for SERS measurement. All the chemicals were used as received without purification. Ultrapure water (18.25 MΩ cm^{-1}, 25 °C) was used throughout the experiments.

Two-dimensional (2D) $Ti_3C_2T_x$ MXene nanosheets were synthesized by using the established minimally intensive layer delamination (MILD) method (Alhabeb et al. 2017). Briefly, 4 g of LiF powder was completely dissolved in

50 mL of 9 M of hydrochloric acid solution with continuous stirring for 10 min at 200 rpm. Then, 2.5 g of Ti_3AlC_2 powder was gradually added into the above etchant solution under a persistent stirring at 380 rpm for 24 h at 35 °C. After the reaction, the mixture was centrifuged at 3500 rpm at 17 °C for 2 min per cycle until a pH above 6 was achieved. This step was repeated for 10–11 cycles. The supernatant was discarded, and the pellet at the bottom was redispersed in water. Handshaking was performed to exfoliate the synthesized $Ti_3C_2T_x$ into few-layer flakes. Two cycles of centrifuging at 100 g for 30 min were performed to remove the unetched Ti_3AlC_2 precursors settled at the bottom of the centrifuge tube. Lastly, the supernatant was collected and further centrifuged at 270 g for 30 min to remove the thick $Ti_3C_2T_x$ flakes. The swollen pellet at the bottom was collected and redispersed in water by very gentle handshaking. The dispersion was then degassed with argon gas for 10 min and stored in fridge (4 °C) for further use.

Garcia-Leis et al.'s approach was used to synthesize the colloidal AgNs by chemical reduction of Ag in two steps (Garcia-Leis et al. 2013). TC was used after using HA, a neutral reducing agent. Briefly, a solution containing of 10 mL HA solution (6×10^{-2} M) and 10 mL of NaOH solution (5×10^{-2} M) was prepared and placed under stirring for 1 min at 200 rpm followed by dropwise addition of 180 mL $AgNO_3$ solution. The solution was stirred at 400 rpm for 5 min. The solution starts to change color from colorless to dark gray. Next, 200 µL of sodium citrate (1% w/v) was added to the mixture. Lastly, the solution mixture underwent a sonication process for 15 min and then the mixture was centrifuged at 6000 rpm for 15 min. The colloidal solution was stored at 4 °C until used.

We fabricated the MXene/AgNs composite via electrostatic interactions and tested them as a SERS substrate for detecting the pesticide thiram as shown in Fig. 1. The composite materials were prepared by mixing the MXene and AgNs dispersions in different volume ratios of 1:5, 5:1, 1:10, 10:1, and 10:10 to determine the optimal volume ratio. Using lower volumes of dispersions did not yield enough material to make complete films and hence poor SERS signals were observed. We added the appropriate volumes of the colloidal AgNs and MXene aqueous solution to prepare the composite and further sonicated the mixture for 15 min. The resulting dispersion was washed and centrifuged to remove excess AgNs and the precipitate was dissolved in 1 mL of deionized water.

In the Raman experiments, a stock solution of thiram with 1 M concentration was prepared by mixing 0.25 g of thiram powder with 1 mL of ethanol solution. Then, this mixture was sonicated for 10 min to ensure it dissolved completely. Lastly, this stock solution was then diluted with ethanol to obtain different concentrations ranging from 10^{-8} M to 10^{-2} M. To prepare the SERS substrates, glass slides were cut into

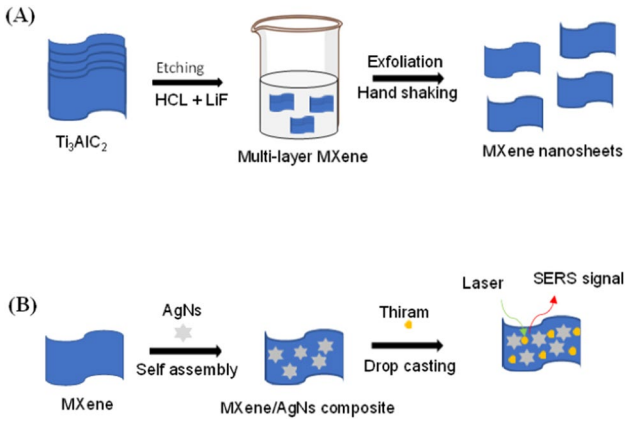

Fig. 1 **A** Schematic illustration of MXene nanosheets' preparation. **B** Schematic design of the MXene/AgNs composite as SERS substrate for thiram detection

1.2 cm × 1.2 cm squares. Then, these glass slides were cleaned by ultrasonication in acetone, propanol, and deionized water sequentially for 15 min per cycle. The colloidal AgNs, aqueous MXene and MXene/AgNs composites solution were deposited on the glass substrate surfaces and dried in vacuum oven at 40 °C. 10 µL of the thiram solution was dropped onto the SERS substrates, and the substrate surfaces were left to air dry for 15 min to ensure sufficient adsorption of the analyte and substrates. The Raman spectra were collected with a 785-nm laser as the excitation source at room temperature. The Raman spectra were acquired in the range of 300–1600 cm^{-1}, and all the spectra were baseline-corrected to exclude the fluorescence background.

The UV–Vis absorption spectra of MXene, AgNs and composites of MXene/AgNs solutions were acquired from the UV-2600 Shimadzu spectrometer with quartz cuvettes at room temperature. The morphologies of these samples were characterized by transmission electron microscopy (TEM) from a Hitachi HT 7700 and by field emission scanning electron microscopy (FE-SEM) from a JEOL JSM-7100F. For elemental composition, EDX analysis of these samples was carried out using JEOL JSM-7100F. SERS measurements were conducted using a Renishaw model InVia micro-Raman spectrometer with a 785 nm wavelength diode laser at 10% power from a 167 mW laser (16.7 mW) using 5 s integration time. The reference spectrum of thiram on bare glass and SERS spectra were collected at 10% power from a 167 mW laser (16.7 mW) using 5 s integration time using 50 × objective with 5 accumulations.

Results and discussion

The structure of the synthesized AgNs was confirmed using TEM with the average diameter being 200 nm as shown in Fig. 2A. Figure 2B shows the structure of delaminated MXene by showing the single layer $Ti_3C_2T_x$ MXene flakes with an average flake size of 2 µm. The structure of the combination of MXene and AgNs in solution with a ratio of 10:10 is displayed in Fig. 2C. Based on the TEM image, we found that there were several AgNs attached to the MXene nanosheet surface in the composite solution. The AgNs can easily assemble around the surface MXene nanosheets because AgNs have positive charges due the presence of surfactant of TC and the surface of MXene is negatively charged due to the surface terminations of hydroxyl and fluoride functional groups (–OH and –F) (Tang et al. 2019). The UV–Vis spectra of the colloidal AgNs, delaminated MXene and various ratios of MXene/AgNs composites are shown in Fig. 2D. A delaminated MXene colloidal solution (black line in Fig. 2D) shows peaks at 260 and 805 nm. According to Satheeshkumar et al., the first absorption band at 260 nm corresponds to the bandgap energy of MXene (Satheeshkumar et al. 2016) while the absorption band at 805 nm may be due to the longitudinal oscillation in delaminated MXene in the near-infrared region. Next, absorption bands at approximately ~ 260 and ~ 384 nm were observed for all volume ratios of MXene/AgNs composites. The absorption band at ~ 260 nm is likely attributed to MXene, whereas the absorption band at ~ 380 nm suggests the existence of AgNs. Dilution of the AgNs or MXene dispersions in making the composites of course lowers the concentration of the species of interest. Using relatively high volumes (compared to the other component) of the AgNs or MXene dispersions ensures a high concentration of that species meaning that the MXene peak at 805 nm is readily observed when the volume ratio favors MXene while the AgNs peak at 384 nm is readily observed in composites formed using volume ratios with more AgNs dispersions. Importantly, the spectrum of the 10:10 dispersion exhibited both these peaks confirming the presence of both species at concentrations that will yield SERS substrates where both species can contribute to the SERS signals observed.

We performed SEM analysis to visualize the morphology of AgNs and MXene as shown in Fig. 3A–B. From the SEM images, we found that the deposited AgNs clusters on the substrate surface have preserved the presence of spikes. The deposited MXene nanosheet on the substrate surface

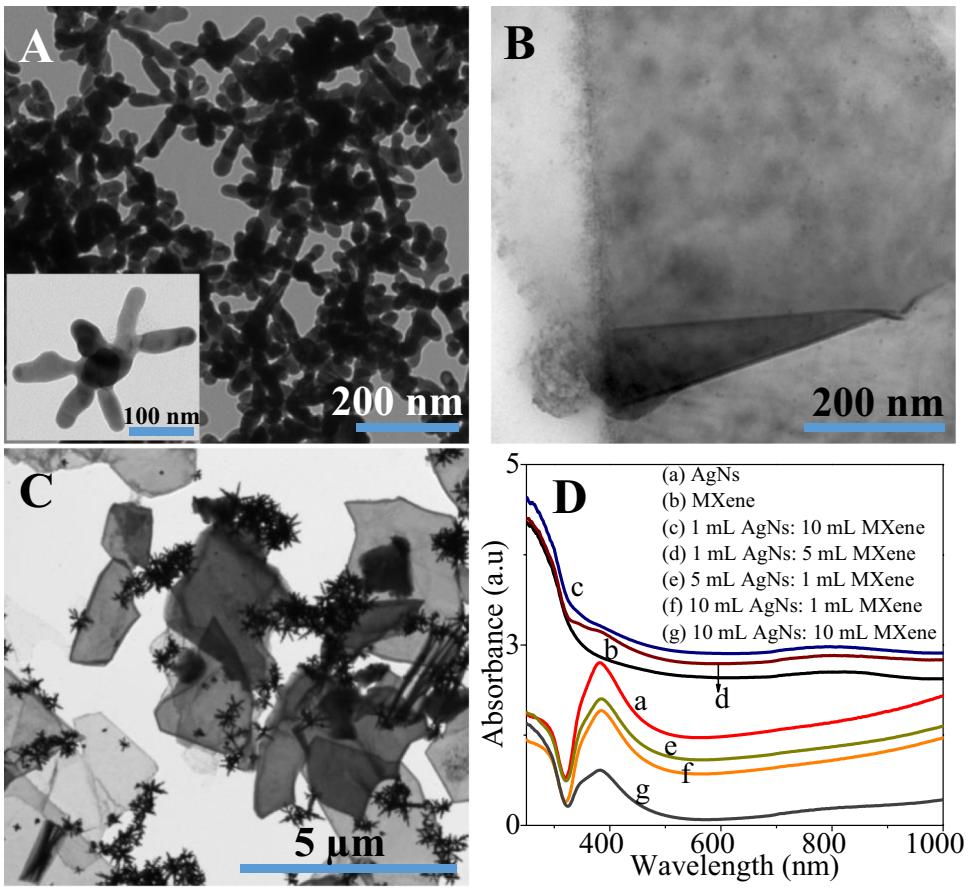

Fig. 2 The TEM images of **A** AgNs, **B** MXene and **C** MXene/AgNs composite with a ratio of 10:10. **D** UV–Vis absorption spectra of colloidal AgNs, MXene solution and various ratios of MXene/AgNs composite solutions

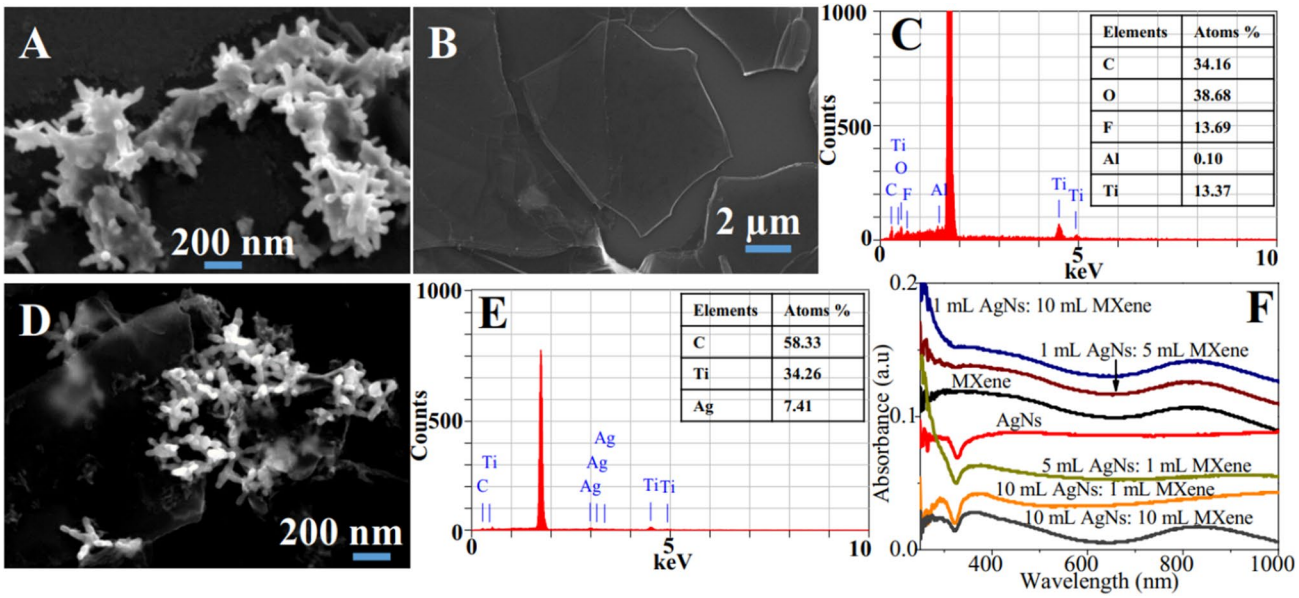

Fig. 3 The thin films characterization **A** SEM image of AgNs, **B** SEM image of MXene, **C** EDX analysis of MXene, **D** SEM image of MXene/AgNs composite with a ratio of 10:10, **E** EDX analysis MXene/AgNs composite with a ratio of 10:10 and **F** UV–Vis absorption spectra of AgNs, MXene and ratios of MXene/AgNs composites

showed the well-defined flakes edges of individual MXene flakes with large surface-to-volume ratio resulting in more active reaction sites and higher chemical activity (Wang et al. 2015). The EDX analysis of the delaminated MXene in Fig. 3C indicates the successful of etching process after removing the Al layer from the Ti_3AlC_2 MAX phase by showing level of detected Al is 0.10%. Based on the SEM image on the combination of MXene and AgNs with a ratio of 10:10, the AgNs particles tend to attach the MXene flakes surface due to opposite charges presence on the AgNs and MXene surface as shown in Fig. 3. We also observed that attachment of AgNs particles around the surface of MXene nanosheets for 1:5, 5:1, 1:10, 10:1 volume ratios as shown in SI, Fig. S1(A)–S4(A). The presence of the AgNs on the MXene surface in MXene/AgNs composites at 10:10 ratio was confirmed by EDX analysis by detecting Ti, C, and Ag as shown in Fig. 3E. The EDX analysis for 1:5, 5:1, 1:10, 10:1 surfaces is provided in SI, Fig. S1(B)–S4(B). From the overall SEM images and EDX analysis observation, increasing the MXene volume in MXene/AgNs composites clearly showed increasing MXene nanosheets on the substrate surface. This is also similar to the increasing of the AgNs volume in MXene/AgNs composites leading to increased presence of AgNs attached on the MXene surface. This increase in the presence of AgNs on the surface with increasing AgNs in the various volume ratios is confirmed in the detected atomic percentage of the elemental Ti, C and Ag from EDX as shown in SI, Table S1. Absorption spectra of the thin films in Fig. 3F agreed with the distribution of AgNs and MXene on the substrate surface by clearly showing the band at 385 nm for AgNs and 810 nm for MXene. Both peaks can be seen clearly with increasing AgNs and MXene in the composites. Here, MXene/AgNs composite solution with a ratio of 10:10 vividly exhibited both absorbance peaks at 385 and 810 nm. We further studied the optimum thin films surface as SERS substrate for thiram pesticide detection.

The SERS activities of AgNs, MXene and various ratios of MXene/AgNs composites are determined from a simple glass-supported SERS substrate using thiram. Figure 4A depicts the spectra of a 10^{-2} M thiram solution on substrate surfaces containing AgNs, MXene and different volume ratios of MXene to AgNs used to make the MXene/AgNs composite. The presence of the thiram on SERS substrate surface was confirmed by the existence of the nine characteristic peaks at 320, 364, 397, 447, 562, 854, 977, 1376 and 1400 cm^{-1} which were assigned to the S=C–S bending, C–S stretching, S–S stretching, C–S–S deformation, S–S stretching, CH_3–N stretching, C–S–S asymmetric stretching, C–N stretching and C–N stretching modes, respectively (Verma and Soni 2019). These characteristic peaks of thiram match the corresponding peaks of thiram on bare glass. The substrate containing 10 mL AgNs and 10 mL MXene exhibits the strongest SERS signal among the other ratios, MXene and AgNs alone as evidenced in Fig. 4A. Closer examination of Fig. 4A shows that the composites containing 10 mL AgNs and 10 mL MXene give the best SERS signal with the calculated enhancement factor (EF) for the highest band at 562 cm^{-1} being approximately 1.1×10^{3}. The overall calculated EF for AgNs, MXene and MXene/AgNs ratios were described in Table 1. Using the substrate containing 10 mL

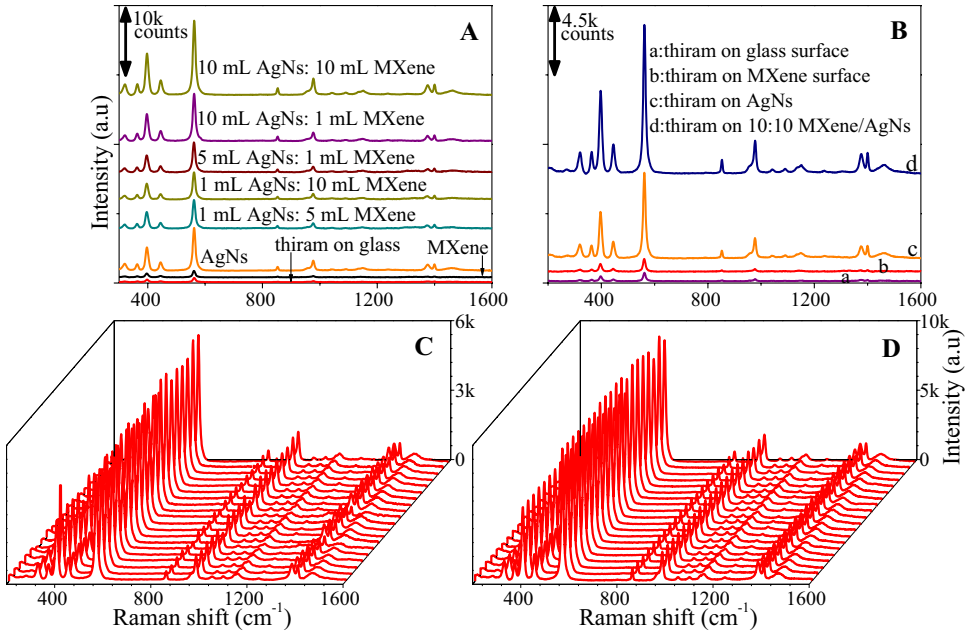

Fig. 4 **A** SERS signals of 10^{-2} M thiram on glass, AgNs, MXene and various ratios of MXene/AgNs composites (spectra offset for clarity). **B** SERS signals of 10^{-2} M thiram on glass, AgNs, MXene and MXene/AgNs composites with a ratio of 10:10 (spectra offset for clarity). **C** Reproducibility of AgNs for 20 different spots and **D** reproducibility of MXene/AgNs with a ratio of 10:10 for 20 different spots

Table 1 The calculated EF for various SERS substrates

SERS substrates	EF
AgNs	6.3×10^{2}
MXene	9.6×10^{1}
10 mL AgNs: 10 mL MXene	1.1×10^{3}
10 mL AgNs: 1 mL MXene	7.0×10^{2}
5 mL AgNs: 1 mL MXene	4.4×10^{2}
1 mL AgNs: 10 mL MXene	4.0×10^{2}
1 mL AgNs: 5 mL MXene	4.2×10^{2}

AgNs and 10 mL MXene ensures that there are significant number of AgNs in the composite but that the AgNs are well spread out and isolated on the MXene yielding the highest availability of hot spots. The suboptimum amounts of AgNs lead to significant clustering, as seen in the SEM images shown the supplemental Fig. S1–S4 which lowers the number of available active hot spots, thus lowering the SERS enhancement. Figure 4B displays the SERS spectra of thiram molecules on three different substrate surfaces namely MXene, AgNs and MXene/AgNs composite with a ratio of 10:10. Both MXene and AgNs substrates exhibit SERS signal from thiram. However, 10^{-2} M thiram signals on the MXene surface are not as strong and very similar to thiram alone on the glass surface. Meanwhile, the thiram signals on AgNs surface are lower than the 10:10 MXene/AgNs substrate. The enhancement in the composite can be attributed to both EM and CM enhancement. The CM enhancement results from the charge transfer and chemical bonding effects between MXene and the thiram pesticide, while the EM enhancement is based on the enhancement of the local electromagnetic field produced by the AgNs hot spots. There are a few EF formulae for EF calculation and here we chose the analytical enhancement factor approach as described by Ru et al. group (Le Ru et al. 2007). These EF values were calculated using Formula 1.

$$\mathrm{EF} = \frac{I_{\mathrm{SERS}}/N_{\mathrm{SERS}}}{I_{\mathrm{Raman}}/N_{\mathrm{Raman}}} \tag{1}$$

where I_{Raman}: Intensity of non-SERS; I_{SERS}: Intensity of SERS; N_{Raman}: Average number of molecule for non-SERS that contributed the signal and N_{SERS}: Average number of molecule for SERS that contributed the signal. The calculation details for EF value have been reported in our previous article (Abu Bakar and Shapter 2023). This EF value proves that the optimum volume ratio of MXene/AgNs composite can be a good SERS substrate compared to MXene and AgNs alone.

As stated earlier, SERS enhancement happens through two mechanisms, namely an electromagnetic (EM) mechanism and a chemical (CM) mechanism (Zhang et al. 2014; Chu et al. 2017; Xia 2018). The EM mechanism is generally observed in substrates rich in free electrons that can generate localized surface plasmon resonance (LSPR) upon excitation (Cong et al. 2020). Due to the variety of terminal groups, MXenes have a very diffuse Fermi level (Ampong et al. 2023) and hence is an ideal candidate to display enhancement through the EM mechanism due to the high density of electrons around the Fermi level. The adsorption of the thiram only increases the variety of terminations which will increase the likelihood of this enhancement. The CM mechanism can have three possible origins in a metal–molecule

system, namely interfacial ground-state charge transfer, the photoinduced charge transfer resonance, and the electronic excitation resonance within the molecule itself (Jensen et al. 2008). See Fig. 5 for the energy levels involved in the SERS system involving AgNs and thiram. In our experiments, the laser wavelength is 1.58 eV while the energy levels of thiram have a LUMO of − 1.53 eV with a HOMO of − 4.72 eV giving a gap of 3.19 eV, and thus resonance Raman of the molecule itself is not possible (Hieu et al. 2021). The Fermi level of AgNPs is generally about − 4.26 eV (Mai et al. 2022) meaning the gap to the LUMO of thiram is 2.73 eV. This is a large gap meaning that photoinduced charge transfer resonance mechanism is unlikely (Mai et al. 2022). The Fermi level of Ag and the HOMO of thiram have very similar energies meaning that the most likely SERS enhancement mechanism interfacial ground-state charge transfer. These ground state interactions change the polarizability of the metal–molecule complex leading to higher Raman cross-sections.

The hybrid systems lead to higher enhancement than just a summation of the two individual enhancements. There are likely several factors leading to this observation. The presence of the MXene reduces the clustering the AgNs providing more available metal nanostructures to enhance the signal. Additionally, yet another termination of the MXene may provide more electron density in the system to enhance the EM mechanism.

Sensitivity is one of the important factor for SERS substrates. However, Raman signal reproducibility and stability are also critical. Since the enhancement factor is highest for 10:10 MXene/AgNs, this system was studied further. The single MXene SERS substrate was not studied further due to its low SERS enhancement. In Fig. 4C–D, 10^{-2} M thiram solution was dropped onto the AgNs and 10:10 MXene/AgNs substrate surfaces, and 20 different spots on the same samples were selected for testing. We analyzed the uniformity of field enhancement of SERS substrate surface by measuring the relative standard deviation (RSD) at three highest characteristic peaks of thiram as shown in SI, Fig. S5. The SERS intensity of each characteristic peak on AgNs showed changes with the calculated RSD of the intensity at 397, 562 and 977 cm^{-1} which were 9.64, 11.12 and 13.54%, respectively. The RSD values on MXene/AgNs surface were lower at 3.07, 3.55 and 2.87% for 397, 562 and 977 cm^{-1}, respectively. We also explored the reproducibility properties of SERS substrates on 20 different samples with the corresponding full spectra of SERS signal and RSD measurements shown in SI, Fig. S6. The SERS intensity of each characteristic peak showed only slight changes for MXene/AgNs compared to AgNs alone, as demonstrated by the RSD of the intensity at 397, 562 and 977 cm^{-1} which were 2.22, 2.55 and 2.50%, respectively. Meanwhile, the RSD value for AgNs are 7.30, 8.46 and 11.32% for bands at 397, 562 and 977 cm^{-1}, respectively. These findings suggest that the MXene/AgNs substrate exhibits excellent reproducibility.

To investigate the potential application of the AgNs and 10:10 MXene/AgNs ratio as SERS substrates, we prepared the substrate and evaluated it using thiram solutions with

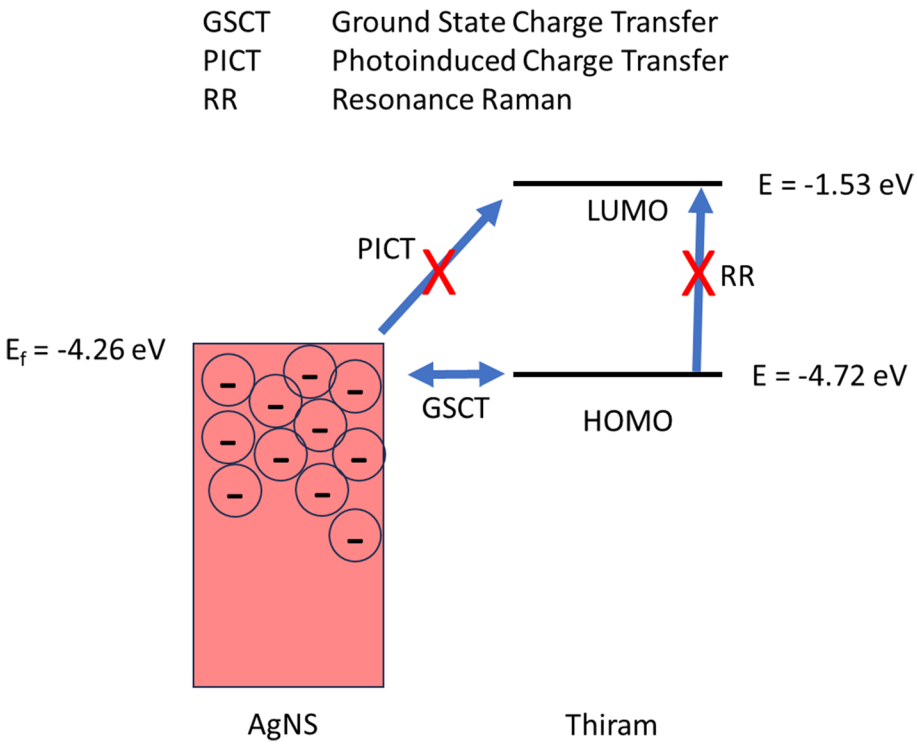

Fig. 5 Energy levels involved in the SERS enhancement of thiram on a AgNs substrate

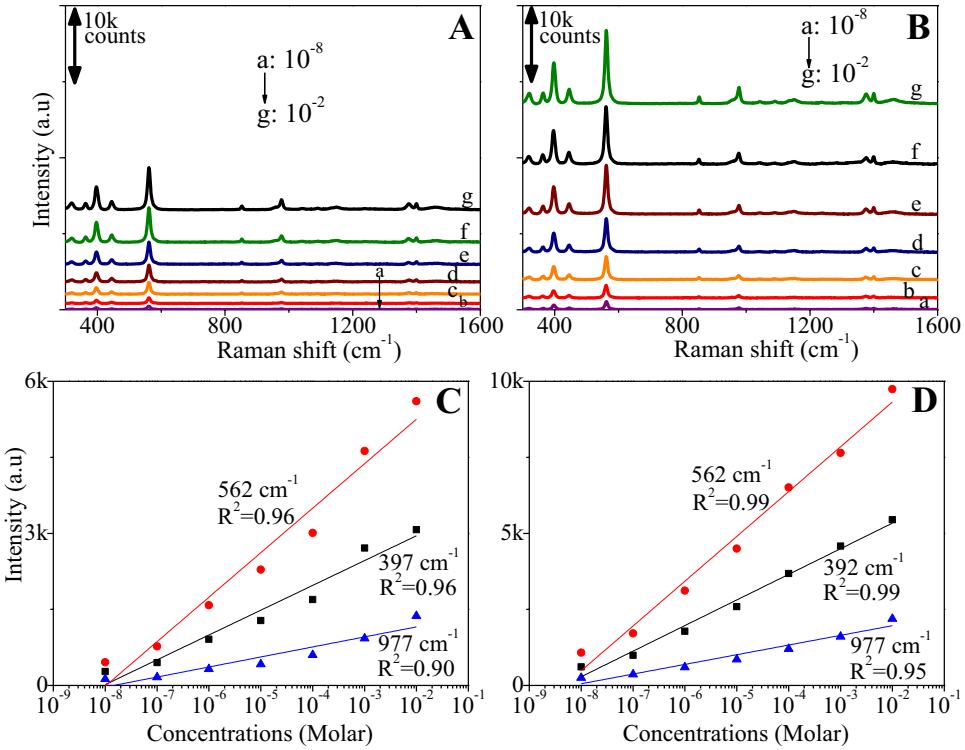

Fig. 6 SERS spectra of different concentrations of thiram on **A** AgNs and **B** 10:10 MXene/AgNs ratio (spectra offset for clarity). The corresponding relationship between intensity and different concentrations (10^{-8} to 10^{-2} M) of thiram detected by **C** AgNs and **D** MXene/AgNs SERS substrates

different concentrations of 10^{-2}, 10^{-3}, 10^{-4}, 10^{-5}, 10^{-6}, 10^{-7} and 10^{-8} M. As presented in Fig. 6A–B, the intensity of the characteristic peak increased with increasing thiram concentration on the SERS substrate surfaces as expected. Thiram signal is higher on composite surface than those signals on AgNs only surface for the seven concentrations. The characteristic peaks of thiram are still observable at the lowest concentration on the AgNs and composite surfaces. Moreover, we further conducted a quantitative analysis of the characteristic peaks at 397, 562 and 977 cm^{-1}, by studying the log relationship between SERS intensity and concentrations as demonstrated in Fig. 6C–D. It was found that AgNs and composite surfaces have good correlations as high as 0.96 and 0.99, respectively, for the bands at 397 and 562 cm^{-1}. From these results, we calculated the limit of detection (LOD) for detection of thiram on AgNs and MXene/AgNs surfaces which were 2.1×10^{-8} M and 7.6×10^{-9} M, respectively. Therefore, the results indicate that the MXene/AgNs substrates exhibited higher sensitivity than single AgNs and could be used to estimate pesticide residue in the environment and food products.

The study proceeded to examine the stability of the AgNs and MXene/AgNs substrates in air after a storage period of 1 month in a small transparent container with silica gel. A

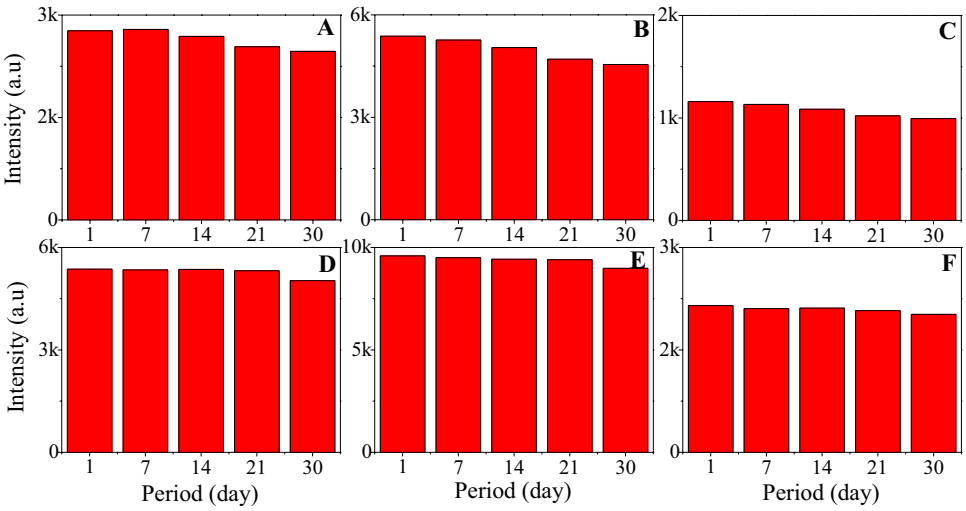

Fig. 7 Histogram of intensity and storage time distribution for AgNs substrate with 10^{-2} M thiram adsorbed at **A** 397 cm^{-1}, **B** 562 cm^{-1}, **C** 977 cm^{-1}. Histogram of intensity and storage time distribution for MXene/AgNs substrate with a ratio of 10:10 with 10^{-2} M thiram adsorbed at **D** 397 cm^{-1}, **E** 562 cm^{-1}, **F** 977 cm^{-1}

reliable SERS substrate should maintain its properties even after being stored in air for an extended period. Figure 7 illustrates the corresponding SERS intensity of the 397, 562 and 977 cm^{-1} bands for 10^{-2} M thiram during the storage period. The peaks' position and intensity did not show significant changes indicating that the substrate exhibited good stability. The thiram signals appeared to slightly decrease over storage time, however the RSD value for the decreasing SERS signals remain low. The calculated RSD value for AgNs surface are 5.38, 7.13 and 6.58% for 397, 562 and 977 cm^{-1} peaks, respectively. It was found that the presence of MXene in composite surface as SERS substrate can enhance the stability surface over time with RSD values of 2.71, 2.48 and 2.28% for 397, 562 and 977 cm^{-1} peaks, respectively. The full stability spectra of SERS and RSD measurements are provided in SI, Fig. S7.

There have been various approaches using SERS to detect thiram with LODs ranging from 2×10^{-6} M to 10^{-12} M (Zhu et al. 2017; Kumar and Soni 2020; Xiao et al. 2023). The utilization of silver nanostars SERS detection for thiram has previously been observed using multi-spike silver stars (Verma and Soni 2019). An LOD of 6.3×10^{-7} M for thiram using multibranched Au–Ag bimettalic nanostars SERS substrates has been reported (Li et al. 2018). Other research studies using silver coated gold nanostars give limits of detection ranging from of 0.8 to 5×10^{-9} M (Rathod et al. 2022; Atta and Vo-Dinh 2022). The combination of MXene and gold nanorods (MXene/AuNRs) has been reported to detect thiram with a limit of detection of 10^{-8} M and 10^{-10} M (Xie et al. 2019; Wang et al. 2021), similar to the limit of detection in this study at 7.6×10^{-9} M after introducing MXene into silver nanostars structure to detect thiram. Thiram detected using AgNs and MXene/AgNs SERS substrates in this article is notably lower than the current concentration permissible as set by U.S Environmental Protection Agency set at 2.91×10^{-5} M, by European Union at 4.16×10^{-7} M-4.16×10^{-6} M, by Argentina National Service of Sanitation and Agri-Food Quality at 4.16×10^{-6} M-1.25×10^{-5} M (Picone et al. 2022). The reproducibility towards detection of thiram on MXene/AgNs surface confirmed the low RSD value of less than 4% while the RSD values on MXene/AuNRs were around 7% (Wang et al. 2021) and 10% (Xie et al. 2019). Unlike other previous research efforts, we have measured the stability of MXene/AgNs as a SERS substrate over a storage time of a 1 month. This stability will be critical in situations where remote sampling might be required and substrates are then shipped for measurement.

Conclusions

In summary, various substrates were successfully fabricated through a simple electrostatic interaction. The MXene/AgNs substrate displayed superior SERS activity compared to either the MXene only or AgNs only substrates and the optimal ratio of MXene to AgNs dispersion was determined. The optimal MXene/AgNs composite was used to detect thiram pesticide at various concentrations ranging from 10^{-8} to 10^{-2} M. The results indicated a linear correlation between the peak intensity and concentration, highlighting its potential for environmental analysis. Notably, the substrate exhibited good reproducibility, which is a crucial characteristic for any detection technique. Additionally, the study highlighted the substrate's long-term stability, indicating that it could be used effectively over an extended period without significant loss of performance or degradation. These positive findings suggest that MXene/AgNs substrate holds potential as a cost-effective and practical option for detection applications.

Supplementary Information The online version contains supplementary material available at https://doi.org/10.1007/s11696-023-03276-3.

Acknowledgements Norhayati Abu Bakar would like to thank Ministry of Higher Education Malaysia and Universiti Kebangsaan Malaysia for her fellowship. This work was supported by the Australian Research Council (DP200101217). This work was performed in part at the Queensland node of the Australian National Fabrication Facility, a company established under the National Collaborative Research Infrastructure Strategy to provide nano- and micro-fabrication facilities for Australia's researchers. This characterisation work was supported by Centre for Research and Instrumentation Management (CRIM), Universiti Kebangsaan Malaysia and Centre for Microscopy and Microanalysis (CMM), University of Queensland.

Funding Open Access funding enabled and organized by CAUL and its Member Institutions.

Availability of data and materials Data will be made available on request.

Declarations

Conflict of interest The authors declare no conflict of interest.

References

Abu Bakar N, Shapter JG (2023) Silver nanostar films for surface-enhanced Raman spectroscopy (SERS) of the pesticide imidacloprid. Heliyon 9:e14686. https://doi.org/10.1016/j.heliyon.2023.e14686

Alhabeb M, Maleski K, Anasori B, Lelyukh P, Clark L, Sin S, Gogotsi Y (2017) Guidelines for synthesis and processing of two-dimensional titanium carbide (Ti3C2Tx MXene). Chem Mater 29:7633–7644. https://doi.org/10.1021/acs.chemmater.7b02847

Ampong DN, Agyekum E, Agyemang FO, Mensah-Darkwa K, Andrews A, Kumar A, Gupta RK (2023) MXene: fundamentals to applications in electrochemical energy storage. Discov Nano 18:3. https://doi.org/10.1186/s11671-023-03786-9

Atta S, Vo-Dinh T (2022) Bimetallic gold nanostars having high aspect ratio spikes for sensitive surface-enhanced raman scattering sensing. ACS Appl Nano Mater 5:12562–12570. https://doi.org/10.1021/acsanm.2c02234

Barveen NR, Wang T-J, Chang Y-H (2021) A photochemical approach to anchor Au NPs on MXene as a prominent SERS substrate for ultrasensitive detection of chlorpromazine. Microchim Acta 189:16. https://doi.org/10.1007/s00604-021-05118-z

Bhavya MB, Prabhu BR, Shenoy BM, Bhol P, Swain S, Saxena M, John NS, Hegde G, Samal AK (2020) Femtomolar detection of thiram via SERS using silver nanocubes as an efficient substrate. Environ Sci Nano 7:3999–4009. https://doi.org/10.1039/D0EN01049A

Chang P-L, Hsieh M-M, Chiu T-C (2016) Recent advances in the determination of pesticides in environmental samples by capillary electrophoresis. Int J Environ Res Public Health, p 13

Chu HO, Song S, Li C, Gibson D (2017) Surface enhanced Raman scattering substrates made by oblique angle deposition: methods and applications. Coatings 7

Cong S, Liu X, Jiang Y, Zhang W, Zhao Z (2020) Surface enhanced Raman scattering revealed by interfacial charge-transfer transitions. Innov, 1

Dao TC, Luong TQN, Cao TA, Kieu NM (2019) High-sensitive SERS detection of thiram with silver nanodendrites substrate. Adv Nat Sci Nanosci Nanotechnol 10:25012. https://doi.org/10.1088/2043-6254/ab2245

Garcia-Leis A, Garcia-Ramos JV, Sanchez-Cortes S (2013) Silver nanostars with high SERS performance. J Phys Chem C 117:7791–7795. https://doi.org/10.1021/jp401737y

Garg R, Agarwal A, Agarwal M (2020) A review on MXene for energy storage application: effect of interlayer distance. Mater Res Express 7:22001. https://doi.org/10.1088/2053-1591/ab750d

Guo P, Sikdar D, Huang X, Si KJ, Xiong W, Gong S, Yap LW, Premaratne M, Cheng W (2015) Plasmonic core–shell nanoparticles for SERS detection of the pesticide thiram: size- and shape-dependent Raman enhancement. Nanoscale 7:2862–2868. https://doi.org/10.1039/C4NR06429A

Hieu TD, Chinh NT, Nhung NTA, Quang DT, Quang DD (2021) SERS chemical enhancement by copper—nanostructures: theoretical study of Thiram pesticide adsorbed on Cu20 cluster. Vietnam J Chem 59:159–166. https://doi.org/10.1002/vjch.202000137

Jensen L, Aikens CM, Schatz GC (2008) Electronic structure methods for studying surface-enhanced Raman scattering. Chem Soc Rev 37:1061–1073

Kumar G, Soni RK (2020) Silver nanocube- and nanowire-based SERS substrates for ultra-low detection of PATP and thiram molecules. Plasmonics 15:1577–1589. https://doi.org/10.1007/s11468-020-01172-0

Le Ru EC, Blackie E, Meyer M, Etchegoin PG (2007) Surface enhanced Raman scattering enhancement factors: a comprehensive study. J Phys Chem C 111:13794–13803. https://doi.org/10.1021/jp0687908

Li J-J, Wu C, Zhao J, Weng G-J, Zhu J, Zhao J-W (2018) Synthesis and SERS activity of super-multibranched AuAg nanostructure via silver coating-induced aggregation of nanostars. Spectrochim Acta Part A Mol Biomol Spectrosc 204:380–387. https://doi.org/10.1016/j.saa.2018.06.080

Lim SS, Allen K, Bhutta ZA, Dandona L, Forouzanfar MH, Fullman N, Murray CJL et al (2016) Measuring the health-related sustainable development goals in 188 countries: a baseline analysis from the Global Burden of Disease Study 2015. Lancet 388:1813–1850. https://doi.org/10.1016/S0140-6736(16)31467-2

Liu J, Si T, Zhang L, Zhang Z (2019) Mussel-inspired fabrication of SERS swabs for highly sensitive and conformal rapid detection of thiram bactericides. Nanomaterials, p 9

Llorent-Martínez EJ, Ortega-Barrales P, Fernández-de Córdova ML, Ruiz-Medina A (2011) Trends in flow-based analytical methods applied to pesticide detection: a review. Anal Chim Acta 684:30–39. https://doi.org/10.1016/j.aca.2010.10.036

Bhavvya MB, Prabhu B, Tripathi R, Yadav A, John NS, Thapa R, Altaee A, Saxena M, Samal AK (2022) A unique bridging facet assembly of gold nanorods for the detection of thiram through surface-enhanced Raman scattering. ACS Sustain Chem Eng 10:7330–7340. https://doi.org/10.1021/acssuschemeng.2c01089

Mai QD, Nguyen HA, Phung TLH, Xuan Dinh N, Tran QH, Doan TQ, Le A-T (2022) Silver nanoparticles-based SERS platform towards detecting chloramphenicol and amoxicillin: an experimental insight into the role of HOMO–LUMO energy levels of the analyte in the SERS signal and charge transfer process. J Phys Chem C 126:7778–7790

Picone AL, Rizzato ML, Lusi AR, Romano RM (2022) Stamplike flexible SERS substrate for in-situ rapid detection of thiram residues in fruits and vegetables. Food Chem 373:131570. https://doi.org/10.1016/j.foodchem.2021.131570

Qing Li Q, Loganath A, Seng Chong Y, Tan J, Philip Obbard J (2006) Persistent organic pollutants and adverse health effects in humans. J Toxicol Environ Heal Part A 69:1987–2005. https://doi.org/10.1080/15287390600751447

Rathod J, Byram C, Kanaka RK, Sree Satya Bharati M, Banerjee D, Akkanaboina M, Soma VR (2022) Hybrid surface-enhanced raman scattering substrates for the trace detection of ammonium nitrate, thiram, and nile blue. ACS Omega 7:15969–15981. https://doi.org/10.1021/acsomega.2c01095

Sarycheva A, Makaryan T, Maleski K, Satheeshkumar E, Melikyan A, Minassian H, Yoshimura M, Gogotsi Y (2017) Two-dimensional titanium carbide (MXene) as surface-enhanced Raman scattering substrate. J Phys Chem C 121:19983–19988. https://doi.org/10.1021/acs.jpcc.7b08180

Satheeshkumar E, Makaryan T, Melikyan A, Minassian H, Gogotsi Y, Yoshimura M (2016) One-step solution processing of Ag, Au and Pd@MXene hybrids for SERS. Sci Rep 6:32049. https://doi.org/10.1038/srep32049

Shafi M, Duan P, Liu W, Zhang W, Zhang C, Hu X, Zha Z, Liu R, Liu C, Jiang S, Man B, Liu M (2022) SERS sensing using graphene-covered silver nanoparticles and metamaterials for the detection of thiram in soil. Langmuir 38:16183–16193. https://doi.org/10.1021/acs.langmuir.2c02941

Shevchuk K, Sarycheva A, Gogotsi Y (2022) Evaluation of two-dimensional transition-metal carbides and carbonitrides (MXenes) for SERS substrates. MRS Bull 47:545–554. https://doi.org/10.1557/s43577-022-00276-8

Tang H, Feng H, Wang H, Wan X, Liang J, Chen Y (2019) Highly conducting MXene–Silver nanowire transparent electrodes for flexible organic solar cells. ACS Appl Mater Interfaces 11:25330–25337. https://doi.org/10.1021/acsami.9b04113

Uskoković-Marković S, Kuntić V, Bajuk-Bogdanović D, Holclajtner-Antunović I (2017) Surface-enhanced Raman scattering (SERS) biochemical applications. In: Lindon JC, Tranter GE (eds) Koppenaal DWBT-E of S and S, 3rd edn. Academic Press, Oxford, pp 383–388

Verma AK, Soni RK (2019) Silver nanodendrites for ultralow detection of thiram based on surface-enhanced Raman spectroscopy. Nanotechnology 30:385502. https://doi.org/10.1088/1361-6528/ab2845

Wang Z (2021) A Review on MXene: synthesis, properties and applications on alkali metal ion batteries. IOP Conf Ser Earth Environ Sci 714:42030. https://doi.org/10.1088/1755-1315/714/4/042030

Wang H, Wu Y, Zhang J, Li G, Huang H, Zhang X, Jiang Q (2015) Enhancement of the electrical properties of MXene Ti3C2 nanosheets by post-treatments of alkalization and calcination. Mater Lett 160:537–540. https://doi.org/10.1016/j.matlet.2015.08.046

Wang Y, Shen L, Gong Z, Pan J, Zheng X, Xue J (2019) Analytical methods to analyze pesticides and herbicides. Water Environ Res 91:1009–1024. https://doi.org/10.1002/wer.1167

Wang T, Dong P, Zhu C, Gao W, Sha P, Wu Y, Wu X (2021) Fabrication of 2D titanium carbide MXene/Au nanorods as a nanosensor platform for sensitive SERS detection. Ceram Int 47:30082–30090. https://doi.org/10.1016/j.ceramint.2021.07.184

Xia M (2018) A review on applications of two-dimensional materials in surface-enhanced Raman spectroscopy. Spectrosc An Int, pp J 1–9

Xiao L, Feng S, Hua MZ, Lu X (2023) Rapid determination of thiram on apple using a flexible bacterial cellulose-based SERS substrate. Talanta 254:124128. https://doi.org/10.1016/j.talanta.2022.124128

Xie H, Li P, Shao J, Huang H, Chen Y, Jiang Z, Chu PK, Yu X-F (2019) Electrostatic self-assembly of Ti3C2Tx MXene and gold nanorods as an efficient surface-enhanced Raman scattering platform for reliable and high-sensitivity determination of organic pollutants. ACS Sensors 4:2303–2310. https://doi.org/10.1021/acssensors.9b00778

Yuan C, Liu R, Wang S, Han G, Han M-Y, Jiang C, Zhang Z (2011) Single clusters of self-assembled silver nanoparticles for surface-enhanced Raman scattering sensing of a dithiocarbamate fungicide. J Mater Chem 21:16264–16270. https://doi.org/10.1039/C1JM12919H

Zhang Y, Wang Z, Wu L, Pei Y, Chen P, Cui Y (2014) Rapid simultaneous detection of multi-pesticide residues on apple using SERS technique. Analyst 139:5148–5154. https://doi.org/10.1039/C4AN00771A

Zhu J, Chen Q, Kutsanedzie FYH, Yang M, Ouyang Q, Jiang H (2017) Highly sensitive and label-free determination of thiram residue using surface-enhanced Raman spectroscopy (SERS) coupled with paper-based microfluidics. Anal Methods 9:6186–6193

Zhu J, Liu M-J, Li J-J, Li X, Zhao J-W (2018) Multi-branched gold nanostars with fractal structure for SERS detection of the pesticide thiram. Spectrochim Acta Part A Mol Biomol Spectrosc 189:586–593. https://doi.org/10.1016/j.saa.2017.08.074